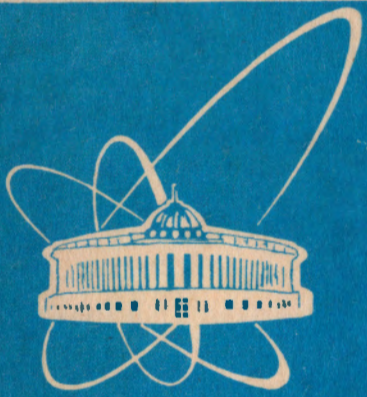

объединенный
институт
ядерных
исследований
дубна

E3-94-403

S.T.Boneva, V.A.Khitrov, A.M.Sukhovoj, A.V.Vojnov

EXCITATION STUDY OF HIGH-LYING STATES OF DIFFERENTLY SHAPED HEAVY NUCLEI BY THE METHOD OF TWO-STEP CASCADES

Submitted to «Nuclear Physics A»

1994

Бонева С.Т. и др.
Е3-94-403

Изучение возбужденных высоколежащих состояний
в тяжелых ядрах различной формы каскадами из двух переходов

Анализируются полученные в последнее время интенсивности двухквантовых γ-каскадов в 14 тяжелых ядрах: ^{137,138,139}Ba, ^{146}Nd, ^{150}Sm, ^{156,158}Gd, ^{160}Tb, ^{164}Dy, ^{168}Er, ^{174}Yb, ^{181}Hf, ^{196}Pt и ^{198}Au. Эксперименты, использующие захват тепловых нейтронов, выполнены преимущественно в Лаборатории нейтронной физики ОИЯИ. Из сопоставления экспериментальных интенсивностей и предсказаний статистической теории выявлены некоторые свойства, связанные с разрядкой компаунд-состояния тяжелого ядра. В сферических ядрах ^{137,138,139}Ba и ^{146}Nd обнаружены очень интенсивные каскады с высокоэнергетическими первичными переходами. Существенно отличается поведение интенсивности каскадов в сильно деформированных ^{156,158}Gd, ^{160}Tb, ^{164}Dy, ^{168}Er и переходном ядре ^{150}Sm, интенсивность первичных переходов с $E_1 \approx 2$—3 МэВ превосходит расчетную величину более, чем на порядок.

Работа выполнена в Лаборатории нейтронной физики ОИЯИ.

Препринт Объединенного института ядерных исследований. Дубна, 1994

Boneva S.T. et al.
E3-94-403

Excitation Study of High-Lying States of Differently Shaped Heavy Nuclei
by the Method of Two-Step Cascades

Recently obtained primary transition intensities from two-step gamma-ray cascade investigation in 14 heavy nuclei: ^{137,138,139}Ba, ^{146}Nd, ^{150}Sm, ^{156,158}Gd, ^{160}Tb, ^{164}Dy, ^{168}Er, ^{174}Yb, ^{181}Hf, ^{196}Pt, ^{198}Au are analysed. Experiments based on thermal neutron capture were undertaken mainly at the Frank Laboratory of Neutron Physics. Comparing these measured intensities and statistical model predictions, some properties of compound-state depopulation were derived. For the spherical nuclei of ^{137,138,139}Ba and ^{146}Nd very intense cascades with high-energy primary transitions were observed. Rather different is the behaviour of the cascade intensity in the strongly deformed nuclei of ^{156,158}Gd, ^{160}Tb, ^{164}Dy, ^{168}Er and in transitional nucleus of ^{150}Sm — intensity of primary gamma-rays with $E_1 \approx 2$—3 MeV overestimates the calculated value by more than one order of magnitude.

The investigation has been performed at the Laboratory of Neutron Physics, JINR.

Preprint of the Joint Institute for Nuclear Research. Dubna, 1994

1 Introduction

For a better understanding of the depopulation mechanism for levels with different energies and structures it is crucial to have information on the dipole radiative widths over a wide region, from low to high energy gamma-rays. A large amount of knowledge has been accumulated from photonuclear reactions and thermal and resonance neutron capture gamma spectroscopy. This information mainly concerns high-energy primary γ-rays that correspond to transitions from the capture states to low-lying levels.

An unambiguous knowledge about the level depopulation mechanism can be deduced from investigations of two-step cascades. Corresponding spectra presenting

γ-ray energy distributions of two-step cascades include the contribution of relatively soft primary gamma transitions proceeding from a high-lying capture state, as well as the contribution of secondary transitions coming from a large number of intermediate levels. It is believed that these spectra may provide indirect but very important information about intermediate energy levels [1].

Over the last ten years in Dubna a method of measuring two-step gamma-ray cascades with a fixed total energy has been developed [2,3]. Up to now the two-step cascade γ-decay spectra of many nuclei from ^{137}Ba to ^{198}Au have been measured and published [4-13]. An important advantage of this method is the opportunity to detect all possible two-step cascades between the compound-state and several low-lying final levels and to extract useful information even in cases where the spaces between decaying states are smaller than the detector resolution. The spectrum of two-step cascades carries information on the photon strength functions that govern the average properties of primary and secondary gamma-ray emission. Analysis of the integral characteristics, such as the total intensity of two-step cascades between levels with known structures, permits some indirect conclusions about their nature. For example, the intensities of two-step cascades exciting the final levels of a single-particle nature in ^{143}Nd, ^{163}Dy, and ^{183}W nuclei are compatible with theoretically predicted values [7]. Analogous intensities exceed, by a factor of 1.5 or more, the values obtained from statistical model predictions in the nuclei of ^{165}Dy, ^{175}Yb, $^{179,181}Hf$, and ^{187}W [1,3]. Such divergence is due to different values of the reduced neutron width Γ_n^0, or to different structures of the neutron resonances. In the first case Γ_n^0 is about $10-20\%$ of the average width $<\Gamma_n^0>$; in the second case it is either equal to or greater than $<\Gamma_n^0>$.

Experiments show that cascades from neutron resonances with large Γ_n^0 mainly excite few-quasiparticle low-lying final states. Those from states with small Γ_n^0 excite many-quasiparticle (collective) high-lying final states of rather complex structures. This result leads to a qualitative explanation [3] of cascade enhancements between compound states with relatively large Γ_n^0 and final states of a pure single-particle nature. Such an explanation supposes the excitation of a system of intermediate levels with reasonable few-quasiparticle components in their wave functions, in the case of the decay of a compound state with a relatively large single-particle component

in its wave function (the case of large Γ_n^0). It also supposes the excitation of a system of levels of a collective nature in cases of small single-particle components in the compound-state structure. A test of the validity of this assumption requires more investigations of two-step cascades for different neutron resonances in the same nucleus.

The set of nuclei presented in this paper belongs to the $4s$-resonance of the neutron strength function where $(\Gamma_n^0/<\Gamma_n^0>)\geq 1$, which ensures almost the same dependence of the process of depopulation on the capturing state properties. Investigation of differently shaped heavy nuclei, spherical as well as deformed, reveals the influence of the shape of the nucleus on the nucleus decay properties at different excitation energies.

2 Experiment and Data Treatment

The Dubna method is based on the usual coincident measurement of two-step cascades that follow thermal neutron capture and end at several final states of known spin and parity. Gamma-gamma coincidences were measured by a spectrometer composed of two back-to-back Ge(Li) or HP(Ge) detectors, having about 10% efficiency. Gamma-rays were detected after passing through a 2.5 g/cm^2 lead filter to minimize the detection of backscattered gamma quanta [2]. To reject coincidences with annihilation quanta, the coincidence detection level was set at 520 keV. In this way, all two-step cascades, through all intermediate states lying 520 keV below the binding energy (B_n) and 520 keV above the excitation energy of the final level E_f, could be detected.

The two-step cascade distributions were obtained [2] using the spectrum of the summed amplitudes of coincident pulses. The peaks in that spectrum are formed by those incidents of γ-detection when the energy of one of the transitions is completely absorbed in one detector and that of the second is completely absorbed in the other detector. Each of these peaks, after appropriate background subtraction, comprises a two-step cascade spectrum. Thus cascade quanta between the capture state and different final levels are registered in different spectra that consist of several components:

1) a set of discrete, experimentally resolved peaks, usually related to high-energy primary γ-transitions that mainly populate the intermediate levels below approximately 3 MeV for deformed and 4 MeV for spherical nuclei.

2) a number of low intensity, experimentally unresolved cascade quanta from the same excitation energy interval as in 1).

3) a broad quasi-continuum formed of low-intensity low-energy primary transitions with an energy E_1 smaller or approximately equal to the second transition energy E_2.

The "noise"-line of these spectra has a zero average value and normally distributed intensity fluctuations with respect to the average.

3 Cascade Intensity Modelling

Systematic measurements (Table 1) of two-step cascade intensities $I_{\gamma\gamma}^{exp}$ for some heavy, differently shaped nuclei were carried out in the excitation energy range up to B_n.

The intensity of a single cascade $i_{\gamma\gamma} = \Gamma_{\lambda g}/\Gamma_\lambda \times \Gamma_{gf}/\Gamma_g$ is determined by the partial widths of the cascade transitions between states $\lambda \to g \to f$ and the total-radiative widths Γ of decaying states λ and g. The ratio $\Gamma_{\lambda g}/\Gamma_\lambda$ has the same energy dependence as the partial widths of the primary transitions, $\Gamma_{\lambda g}$, since $\Gamma_\lambda = const$ for the compound-state. Hence, the cascade intensity $\Delta I_{\gamma\gamma}$, where the energy of one of the quanta falls in the interval ΔE_γ, can be written as

$$\Delta i_{\gamma\gamma} = \sum_i^m \Gamma_{\lambda i}/\Gamma_\lambda \times \sum_f^{n_f} \Gamma_{if}/\Gamma_i, \qquad (1)$$

where $m = \int^{\Delta E} \rho(E_i J_i^\pi)\delta E_i$ is the number of intermediate levels in the interval ΔE.

The cascade intensity calculations should be based on level density model predictions (for a certain spin and parity) and on gamma width modelling of states below B_n. Because of the experimental fact that the spin difference between the initial and final levels of detected cascades is $\mid J_\lambda - J_f \mid \leq 2$ - only $E1$, $M1$ and $E2$ transitions were included in the calculations.

In this paper the intensity predictions were obtained according to relatively simple and often used models:

1) for level density - the backshifted Fermi-gas model (BSFG-model) with the parameters specifying the experimental data as in [14].

2) for the $E1$-photon strength function - the standard Lorentzian model [15], with a width that is independent of energy, was employed for the photoabsorbtion cross section after extrapolation to the excitation energy below B_n. In accordance with the Axel-Brink hypothesis, that expression is valid for the ground-state as well as for an excited one. For $M1$ and $E2$ transitions, the single-particle Weiskopff model was used and the relation B($E1$):B($M1$):B($E2$) was adjusted by 7 MeV to the experimental data [16].

As was already mentioned in earlier papers [3], the measured two-step cascade spectrum carries information on the photon strength function that governs the average properties of primary and secondary γ-ray emission and provides an answer concerning level density and energy strength scaling. To investigate the cascade intensity energy dependence one should divide the cascade transitions into primary and secondary components. This problem was already solved for resolved peaks after their placement in the decay scheme. The ordering of unplaced transitions as well as those that are unresolved was made in accordance with certain assumptions (see [7]).

4 Results

Figs.1-4 present the dependence of intensity distribution on primary transition energy. The histogram shows the experimental data - two-quanta cascade intensities summed in 500 keV energy bins. The modelled values are represented by lines. Table 1 summarizes the investigated nuclei with their binding energy and spin (B_n, J^π), number of final levels - n_f, i.e., the number of observed two-step cascade intensity spectra integrated over all intermediate and final level intensities $I_{\gamma\gamma}^{exp}$ and other parameters.

Due to the low efficiency of the detectors only cascades which have a primary transition intensity of more than 0.01-0.05% of the whole spectrum intensity per decay could be detected. This minimum value of resolved cascade intensity is considered as the lower limit of our spectrometer sensitivity - L_s. For the majority of experimentally

unresolved cascades it is true that the primary transitions have soft energies. But for some other unresolved cascades, the ordering of the cascade quanta is probably determined incorrectly.

Taking into account the available information on decay modes and level schemes, as well as the two-step cascade results, an energy E^* could be set for each nucleus. E^* divides the energy interval between B_n and E_f into two parts - levels below E^* are populated mainly by well resolved cascade transitions, and above E^* the information of cascade intensity is contained in many unresolved transitions. Hence the accuracy (Figs.1-4) of the obtained cascade intensity dependence on the primary ray's energy is limited by the level of equipment sensitivity - L_s. The L_s values for the equipment used are given in Table 1.

At the present time experimental cascade intensity distributions are decomposed into primary and secondary transition components in the following manner [7]:

1) Peaks related to the detection of high energy and intense transitions populating levels below E^* are included in the primary transition two-step cascade intensity distribution. For unresolved parts of the spectra in this energy region, it has been assumed that the low-energy transition is the primary one and the high-energy one is the secondary.

2) For levels from the interval $E^* \leq Eg \leq (B_n - E^*)$ half of the transition intensity is ascribed to primary and half to secondary cascade transitions.

It is necessary to estimate the probable influence of this uncertainty on the shape of the primary transition intensity distribution. As was seen from Table 1, for different nuclei, we were able to observe a rather different portion of the total radiative width of the compound-state as two-step cascades - from 12% to 100%. The fraction of cascades resolved experimentally in the form of pairs of peaks amounts to at least 50-70% or more of the total sum of the observed intensity ($\Delta i_{\gamma\gamma}^{resolved}$ in Table 2). The remaining 30% (or at most 50%) of the total cascade intensity is formed by continuous distribution. The problem of systematic error in the decomposition procedure reduces to the question of how reliable is the decay scheme for the intermediate level energies $E_g < (3-4)$ MeV determined by this method. The studies [17] showed that at an excitation energy below $B_n/2$ the probability of incorrect determination of the quanta ordering in intense cascades is fairly low.

Table 1. Some main properties of the nuclei studied: B_n, J^π - binding energy and spin of the compound state; n_f - number of detected two-quanta intensity distributions; $I_{\gamma\gamma}^{exp}$ - total observed intensity of all spectra; L_s - registration threshold for the equipment used; n_i^{exp} - number of experimentally revealed levels up to 3 MeV; n_i^{cal} - number of levels populated by $E1$-primary transitions in accordance with the BSFG-model in the same energy interval.

Compound nucleus	B_n, J^π MeV	n_f	$I_{\gamma\gamma}^{exp}$ % per decay	L_s % per decay	n_i^{exp}	n_i^{cal}	Ref
^{137}Ba	6.9, $1/2^+$	4	81(3)	0.04	15	17	4
^{138}Ba	8.6, 2^+	2	26(1)	0.03	11	3	5
^{139}Ba	4.7, $1/2^+$	3	100(4)	0.04	18	16	6
^{146}Nd	7.6, 3^-	4	36(1)	0.02	62	13	7
^{150}Sm	8.0, 4^-	6	20(2)	0.01	71	96	8
^{156}Gd	8.5, 2^-	5	32(2)	0.02	72	155	9
^{158}Gd	7.9, 2^-	3	19(1)	0.02	62	116	10
^{160}Tb	6.4, $2^+, 3^+$	12	22(1)	0.01	87	1790	
^{164}Dy	7.7, $2^-, 3^-$	6	46(2)	0.03	64	240	11
^{168}Er	7.8, $3^+, 4^+$	3	15(2)	0.01	59	126	
^{174}Yb	7.5, $2^-, 3^-$	3	22(1)	0.02	72	82	7
^{181}Hf	5.7, $1/2^+$	5	52(4)	0.04	106	263	12
^{196}Pt	7.9, 2^-	3	32(2)	0.05	54	25	13
^{198}Au	6.5, 2^+	19	41(1)	0.01	213	480	

Table 2. Some parameters used in determining the energy scaling of the primary transition intensity.

Compound nucleus	n'_f	$I'_{\gamma\gamma}$ % per decay	E^* MeV	$\Delta i^{middle}_{\gamma\gamma}$ % per decay	$\Delta i^{resolved}_{\gamma\gamma}$ % per decay	$\delta i_{\gamma\gamma}$ *)
^{137}Ba	2	77(3)	3.0	0	71.0	15
^{138}Ba	2	26(1)	4.0	0	21.6	
^{139}Ba	3	100(4)	2.3	0	83.0	15
^{146}Nd	1	20(1)	3.1	3.45	15.6	
^{150}Sm	2	13(1)	3.1	3.76	6.7	16
^{156}Gd	3	23(1)	3.1	5.22	13.1	25
^{158}Gd	3	19(1)	3.0	2.71	12.1	20
^{160}Tb	12	22(1)	2.0	12.8	8.4	
^{164}Dy	3	29(1)	3.0	7.17	13.8	40
^{168}Er	3	15(1)	3.0	6.6	7.2	24
^{174}Yb	3	22(1)	3.0	6.91	12.7	15
^{181}Hf	5	52(4)	2.5	10.58	36.7	
^{196}Pt	3	32(2)	3.3	2.05	29.8	
^{198}Au	19	41(1)	3.0	1.61	30.0	

*) upper limit of intensity error by quanta ordering in % of only part of the spectra area in the energy region $2 \leq E_1 \leq 3$ MeV.

Table 3. Comparison of parameters for ^{160}Tb and ^{198}Au.

Nucleus	B_n, J^π_λ MeV	$< D >$ eV	J^π_f final levels	Probable quanta multipolarity	Γ_λ meV	$\Gamma^o_n / < \Gamma^o_n >$
^{160}Tb	6.375,2^+	3.9	$1^-, 2^-, 3^-, 4^-$	$E1+M1$	97	14
^{198}Au	6.513,2^+	16.5	$1^-, 2^-, 3^-, 4^-$	$E1+M1$	128	3.3

There is no difficulty in subtracting several tens of narrow (several keV) peaks from the experimental intensity distributions. Naturally, the accuracy of this procedure depends on the quality of the spectrum, i.e., on the "noise" fluctuations related to the background subtraction procedure [7] to obtain the cascade intensity distributions. That is the reason for excluding some two-step cascade spectra when decomposing the distribution into two components. For instance, in the ^{146}Nd nucleus only cascades to the first excited 2^+ states are considered. Table 2 contains some information used to obtain the shown (Figs.1-4) cascade intensity dependence on the primary transition energy E_1, namely, n'_f - the number of decomposed two-step cascade spectra; $I'_{\gamma\gamma}$ - the total intensity of these spectra; E^* - the excited state energy dividing all spectra in two parts; $\Delta i^{middle}_{\gamma\gamma}$ - the area of all decomposed cascade spectra in the energy interval $E^* < E_g < B_n - E^*$; and $\Delta i^{resolved}_{\gamma\gamma}$ - that part of the cascade intensity which includes contributions from all resolved cascade transitions.

It is eyident that the interval $E^* < E_g < B_n - E^*$ is narrow and contains no more than $20 - 30\%$ of the total intensity and the posible inaccuracy is not significant. It should be noted that this interval is situated in the middle of the two-step cascade spectrum, and the energy of both primary and secondary γ-transitions is approximatelly equal; dividing it into halves seems reasonable.

A more considerable systematic error could be connected with the assumption about the unresolved part of cascades populating intermediate states below E^* ($E_1 > B_n - E^*$). From Table 1 it can be seen that in the spherical nuclei $^{137,138,139}Ba$ and ^{146}Nd and the nondeformed nucleus of ^{196}Pt, almost all levels below 3 MeV predicted by the BSFG-model were observed and their resolved cascades placed. In that case, for the unresolved peaks, the reliable assumption is that the low-energy transition is the primary one.

In the deformed nuclei of $^{156,158}Gd$, ^{164}Dy and ^{168}Er, only $30 - 50\%$ of the model [14] levels (n^{cal}_i) were experimentally observed. So up to half of their predicted two-step cascades are included in corresponding two-step cascade spectra as broad unresolved quasicontinua. It should be noted, that the most intensive part of the cascades is resolved and this quasicontinuum part carries less information on cascade intensity. For that residual unresolved part divided by the assumption that the low-energy transition is primary, any systematic error should be correctly taken into account.

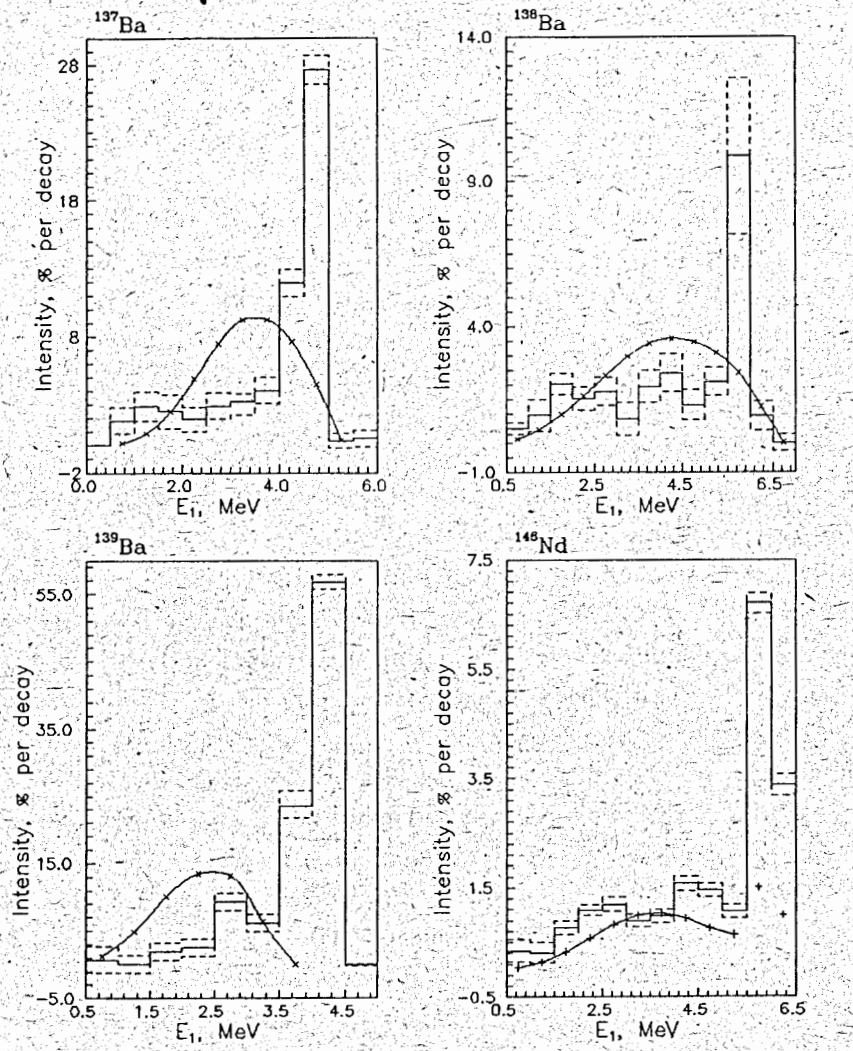

Fig.1. Distribution of total two-step cascade intensities (in % per decay) as a function of primary transition energy, for the spherical nuclei $^{137,138,139}Ba$ and ^{146}Nd. The histogram represents the experimental intensities summed in energy bins of 500 keV; the statistical errors are shown. Curve corresponds to the BSFG-model predictions.

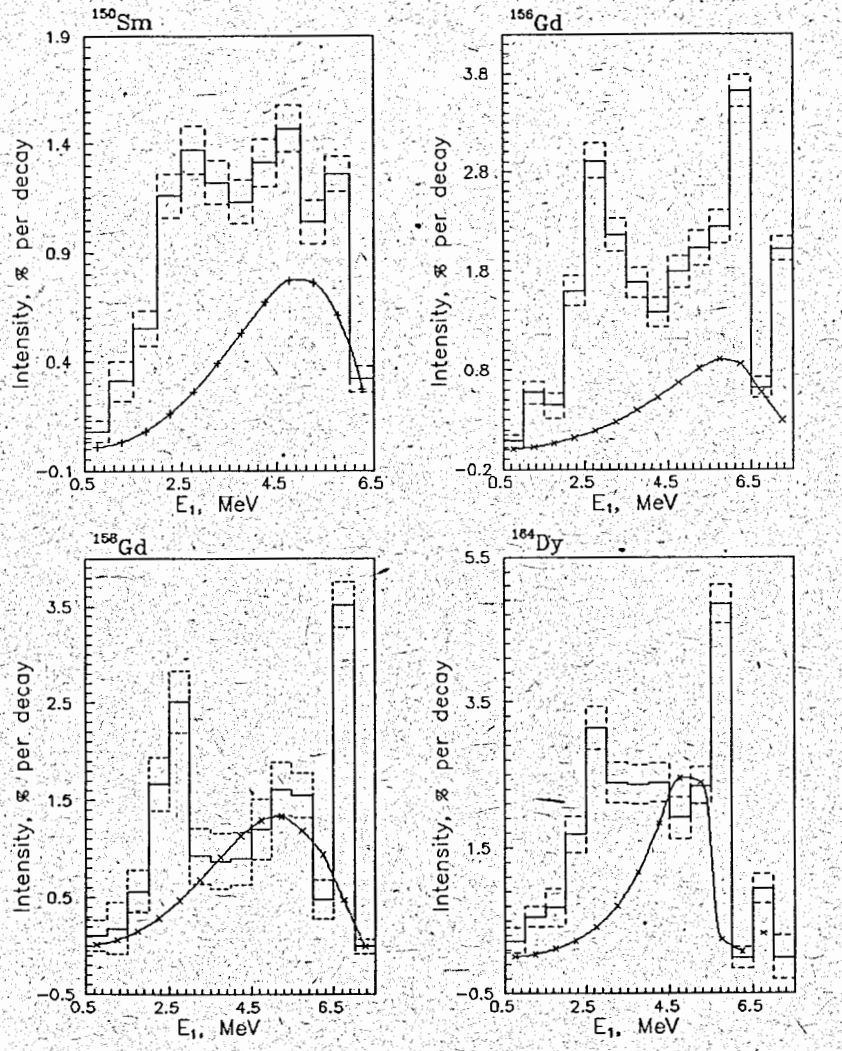

Fig.2. Intensity distribution for ^{150}Sm, $^{156,158}Gd$ and ^{164}Dy nuclei. The notations are the same as in Fig.1.

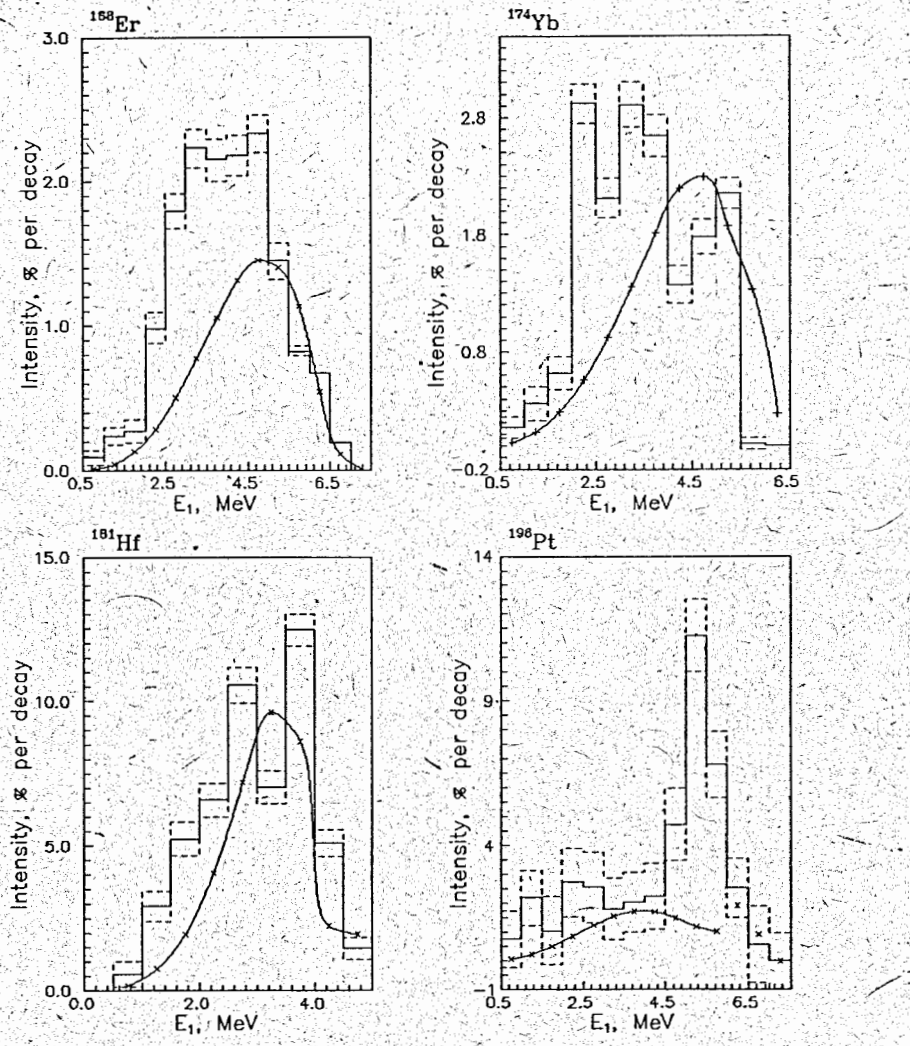

Fig.3. Intensity distribution for ^{168}Er, ^{174}Yb, ^{181}Hf and ^{196}Pt nuclei.

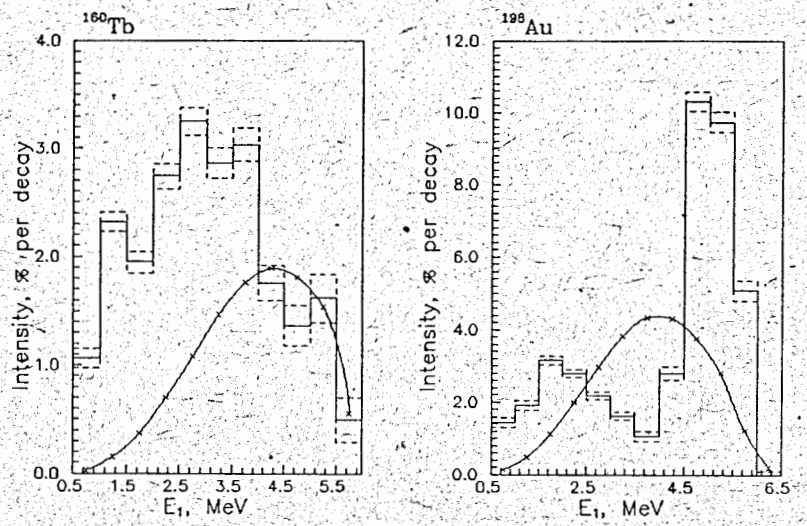

Fig.4. Intensity distribution for ^{160}Tb and ^{198}Au nuclei.

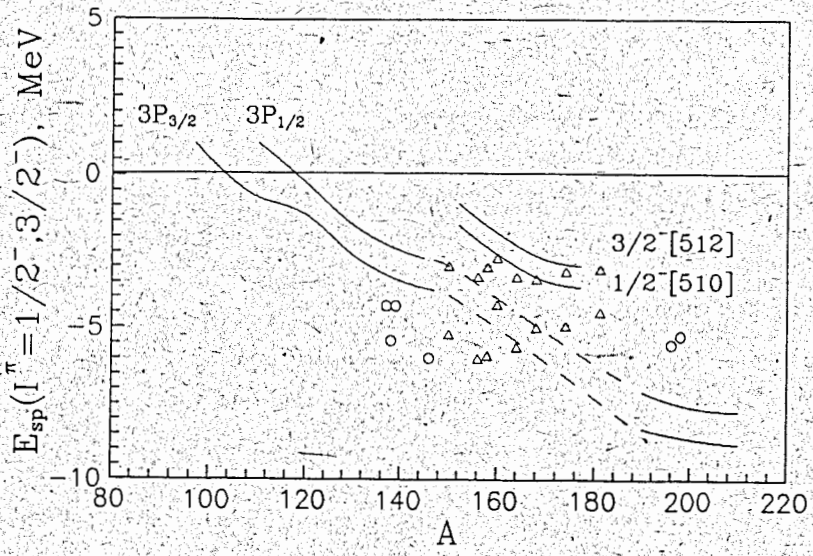

Fig.5. The location of maxima in cascade intensity distributions relative to the neutron binding energy, B_n, versus atomic mass number A. Lines represent the QPNM prediction of single-particle (Woods - Saxon potential) $3p_{1/2}$ and $3p_{3/2}$ states for spherical nuclei and states with $K^\pi = 1/2^-$ and $3/2^-$ for deformed nuclei.

o - the locations of the maximum for spherical nuclei.

Δ - the locations of two maxima in the case of deformed nuclei. The distributions of Fig.3 are decomposed into two peaks, assuming a Lorentzian shape.

Under the acceptable assumptions for $E1$- and $M1$-transition radiative strengths and their Porter-Thomas fluctuations, the error estimation gives its upper limit as $\delta I_{\gamma\gamma}$. That upper limit of spectra decomposition error is present in Table 2 in % of unresolved cascade intensities for the narrow energy interval ($2 < E_1 < 3$ MeV). Such errors are mainly related to weak cascades with primary transition energies $E_1 > B_n - E^*$ falling into the continuous distribution (high level density). That part of all cascade areas is small and does not change the shape of the examined dependence $I^{exp}_{\gamma\gamma} = \mathrm{f}(E_1)$.

5 Discussion and Summary

The intensities of two-step cascades to several low-lying levels of some spherical and deformed nuclei are shown in the form of histograms as a function of their primary transition energy E_1. The calculated cascade intensities (smooth line) of the decomposed spectra are compared with experimental intensities.

The most noticable experimentally revealed feature of compound-state cascade depopulation is "nonstatistical" - the strongly structured shape of the intensity spectra (Figs.1-4). These structural effects appear in different ways for various nuclei. In spherical nuclei the most intense cascades are measured at primary transition energies $E_1 > 4 - 5$ MeV (Fig.1). Low-energy primary transition intensities in those nuclei are comparable with the calculated ones. Another general feature of the $^{137,138,139}Ba$, ^{146}Nd and ^{196}Pt, ^{198}Au nuclei is a relatively large value of Γ^0_n - the reduced neutron resonance width determining the cross section for thermal neutron capture. For these nuclei Γ^0_n is greater than $< \Gamma^0_n >$ [18], the average value over all resonances of the nucleus.

In strongly deformed nuclei from the begining of the $4s$-resonance of the neutron strength function, namely $^{156,158}Gd$ and ^{164}Dy, a second local maximum of intensity distribution was revealed at the primary γ-quanta energy of $E_1 = 2 - 3$ MeV. This intensity enhancement is absent in calculated intensities, because the chosen models predict a smooth energy dependence for level density as well as for gamma strength.

In the ^{160}Tb, ^{168}Er, ^{174}Yb and ^{181}Hf nuclei these two local intensity maxima are

very close and probably create a joint peak, i.e., the greater part of the primary transition intensity falls in the excitation energy region of about $1/2B_n$.

In nuclei from the end of the $4s$-resonance region, ^{196}Pt and ^{198}Au, this second local intensity maximum is not revealed, i.e., there is no significant intensity enhancement at the primary transition energy of $E_1 \sim 3$ MeV. Probably, when increasing the mass number A and changing the shape of the nucleus, the cascade intensity distribution changes its shape as well.

Additional evidence of this hypothessis is the transitional nucleus, ^{150}Sm. The cascade intensity peak at $E_1 = 3$ MeV exists; but it is not as clearly expressed.

For a better understanding of the above mentioned attempt to explain the obtained results by the relation between nucleus shape and the excitation probability of high-lying levels, the ^{160}Tb and ^{198}Au nuclei will be analysed separately. Both nuclei are odd-odd, but the ^{160}Tb nucleus is well deformed and the ^{198}Au nucleus is spherical. Parameters defining capture gamma decay properties, in accordance with modern comprehension, are close for these two nuclei (see Table 3).

Since the odd-odd nucleus has the potential for a great variety of combinations of different quasiparticle excitations, even at low energies, the level densities observed are higher than those seen in neighbouring nuclei (see Table 1). Fig.4 shows a rather different cascade intensity dependence on the excited level energy for these two nuclei. None of the systematic errors nor any statistical errors explain this discrepancy of the principle of obtained cascade intensity at $E_1 \geq 3$ MeV.

The average $4s$-wave resonance spacing $< D >$ differs for these two nuclei and one could expect its influence on the intensity dependence. But the calculated cascade intensity distributions are very close in shape, i.e., in the statistical approach the parameter $< D >$ does not effectively influence the intensity distribution.

Similarity in the shape of the observed dependence $I^{exp}_{\gamma\gamma} = \mathrm{f}(E_1)$ for even-even, even-odd and odd-odd nuclei having the same nucleus shape, and its difference when nuclei differ in shape, permit one to assume that two-step cascade intensities in heavy nuclei depend on the shape of the nucleus.

The difference in the processes of high-energy level population in spherical and deformed nuclei could be connected with the feature of their structure. Among the reasons are strong nonstatistical effects related to the $4s$-maximum of the neutron

strength function. The model calculation [19] shows that the quasiparticle state $510\uparrow$ in the mass region $150 < A < 180$ is situated about 2.5 MeV below B_n (Fig.5). Fig.5 has been taken from paper [19] and shows the QPNM approach to the $3p_{1/2}$ and $3p_{3/2}$ neutron states for spherical nuclei and the $K^\pi = 1/2^-$ and $3/2^-$ states for deformed nuclei. The energy of the $3p$ neutron subshell decreases with increasing mass number A in spherical nuclei. In the region of well deformed nuclei $150 < A < 190$ close to B_n there are single-particle $K^\pi = 1/2^-, 1/3^-$ states. The enhanced transitions in light nuclei are successfully explained in terms of single-particle neutron exchanges between the $3s$ and $2p$ or $3p$ and $3s$ shells [20].

In heavy deformed nuclei the single-particle strength is fragmented and is distributed among many nuclear levels. Thus the contribution of $4s \rightarrow 3p$ transitions to the partial gamma-width is small and not observable by simple detection techniques [21]. The advanced two-step cascade method allows one to see the sum of the transition intensities as an integral characteristic of that fragmented strength, and reveals information on transitions between the $4s$ and $3p$ neutron orbits.

In paper [22] the pronounced local maximum of intensity of primary gamma rays at 2.5 MeV for the ^{156}Gd nucleus was treated as enhanced γ-transitions between the many-quasiparticle components of the capture state and excited states with energies of 5.5-6.5 MeV. Because the experimental data involve only 10^{-6} part of the neutron resonance wave function, it is possible to say that a state whose largest component is described by a single many-quasiparticle configuration (more than 10-20%) has its own characteristic features.

To summarize, the proposed explanation of observed intense cascades via intermediate states lying only 2-3 MeV below B_n is only a hypothesis. Most important are the results of the broad investigation of many heavy nuclei. The two sets of nuclei, generally differing in shape, manifest different forms of cascade intensity distributions as a function of their primary transition energies.

References

[1] S.T. Boneva, V.A. Khitrov, Yu.P. Popov, A.M. Sukhovoj, E.V. Vasilieva, Yu.S. Yazvitsky, Z.Phys. **A(330)** (1988) 153

[2] S.T. Boneva, E.V. Vasilieva, Yu.P. Popov, A.M. Sukhovoj, V.A. Khitrov, Sov. J. Part. Nucl. **22(2)** (1991) 232

[3] S.T. Boneva, E.V. Vasilieva, V.D. Kulik, L.H. Khiem, L.A. Malov, Yu.P. Popov, A.M. Sukhovoj, P.D. Khang, V.A. Khitrov, Yu.V. Kholnov, M.R. Beitins, V.A. Bondarenko, I.L. Kuvaga, P.T. Prokofiev, L.I. Simonova, G.L. Rezvaya, Sov. J. Part. Nucl. **22(6)** (1991) 698

[4] V.A. Bondarenko, I.L. Kuvaga, L.H. Khiem, Yu.P. Popov, P.T. Prokofiev, A.M. Sukhovoj, P.D. Khang, V.A. Khitrov, Yu.V. Kholnov, Izv. RAN, ser. fiz. **55** (1991) 2116

[5] V.A. Bondarenko, I.L Kuvaga, L.H. Khiem, Yu.P. Popov, P.T. Prokofiev, A.M. Sukhovoj, G.L. Rezvaya, L.I. Simonova, P.D. Khang, V.A. Khitrov, Yu.V. Kholnov, Izv. RAN, ser. fiz. **55** (1991) 2088

[6] V.A. Bondarenko, I.L. Kuvaga, L.H. Khiem, Yu.P. Popov, P.T. Prokofiev, A.M. Sukhovoj, P.D. Khang, V.A. Khitrov, Yu.V. Kholnov, Jad. Fiz. **54** (1991) 901

[7] S.T. Boneva, V.A. Khitrov, A.M. Sukhovoj, A.V. Voinov, Z.Phys. **A(338)** (1991) 319

[8] E.V. Vasilieva, A.V. Vojnov, O.D. Kestarova, V.D. Kulik, A.M. Sukhovoj, V.A. Khitrov, Yu.V. Kholnov, V.N. Shilin, Izv. RAN, ser. fiz. **57** (1993) 128

[9] E.V. Vasilieva, A.V. Vojnov, O.D. Kestarova, V.D. Kulik, A.M. Sukhovoj, V.A. Khitrov, Yu.V. Kholnov, V.N. Shilin, Izv. RAN, ser. fiz. **57(10)** (1993) 98

[10] M.A. Ali, A.A. Bogdzel, V.A. Khitrov, Yu.V. Kholnov, V.D. Kulik, L.H. Khiem, N.T. Tuan, P.D. Khang, Yu.P. Popov, V.N. Shilin, A.M. Sukhovoj, E.V. Vasilieva, A.V. Vojnov, JINR preprint E3-91-428 (1991)

[11] E.V. Vasilieva, A.V. Vojnov, O.D. Kestarova, V.D. Kulik, A.M. Sukhovoj, V.A. Khitrov, Yu.V. Kholnov, V.N. Shilin, Izv. RAN, ser. fiz. **57(10)** (1993) 109

[12] V.A. Bondarenko, I.L. Kuvaga, L.H. Khiem, Yu.P. Popov, P.T. Prokofiev, A.M. Sukhovoj, P.D.Khang, V.A. Khitrov, Yu.V. Kholnov, Izv. RAN, ser. fiz. **55** (1991) 2091

[13] M.A. Ali, V.A. Khitrov, Yu.V. Kholnov, O.D Kjostarova, A.M. Sukhovoj, A.V. Vojnov, JINR preprint E3-94-3 (1994)

[14] W. Dilg, W. Schantl, H. Vonach, M. Uhl, Nucl. Phys. **A217** (1973) 269

[15] P. Axel, Phyz. Rev. **126** (1962) 671

[16] J. Kopecky, Proc. 4th Int. Symp. on Capture Gamma-Ray Spectroscopy and Related Topics, Grenoble, 1981, ed. T.von Egidy (Inst. of Phys., Bristol-London, 1982) p.423

[17] M.R. Beitins, S.T. Boneva, V.A. Khitrov, L.A. Malov, Yu.P. Popov, P.T. Prokofiev, G.L. Rezvaya, L.I. Simonova, A.M. Sukhovoj E.V. Vasilieva, Z. Phys. A - Hadrons and Nuclei **341** (1992) 155

[18] S.F. Mughabghab, Neutron Cross Sections 1, Part B. New York: Academic Press, 1984
S.F.Mughabghab, M. Divadeenam, N.E. Holden, Neutron Cross Sections 1, Part A. New York: Academic Press, 1981

[19] V.G. Soloviev, Sov. J. Part. Nucl. **3**(4) (1972) 770

[20] S.F. Mughabghab, R.E. Chrien, Proc. 3rd Int. Symp. on Neutron Capture Gamma-Ray Spectroscopy and Related Topics, New York, 1978, ed. R.E. Chrien, W.E. Kane (Plenum Press, New York and London, 1979) p.265

[21] S.F. Mughabghab, Proc. 2nd Int. Symp. on Neutron Capture Gamma-Ray Spectroscopy and Related Topics, Petten, 1974, ed. K. Abrachams, F. Stecher-Rasmussen, P.van Assche, (Reactor Centrum Nederland, Petten, 1975) p.53

[22] V.G. Soloviev, Proc. 8th Int. Symp. on Capture Gamma-Ray Spectroscopy and Related Topics, Fribourg, 1993, ed. J. Kern (World Scientific, Singapore, 1994) p.103

Received by Publishing Department
on October 17, 1994.